PAPER

Check for updates

pH-sensitive peptide hydrogel encapsulating the anti-angiogenesis drug conbercept and chemotherapeutic drug dox as a combination therapy for retinoblastoma†

Wen Fan,[a] Mingkang Chen,[a] Faisal Raza, [b] Hajra Zafar,[b] Faryal Jahan,[c] Yuejian Chen,[d] Lexin Ge,[a] Minyan Yang*[e] and Yiqun Wu*[f]

Retinoblastoma (RB) is a malignant tumor originating from the retina. Radiotherapy, chemotherapy, photo-dynamic therapy, cryotherapy, and surgery are commonly used in the clinical treatment of RB, but the overall efficacy is poor and often accompanied with tumor metastasis. Vascular endothelial growth factor (VEGF) has been confirmed to be highly expressed in the aqueous humor of RB patients and is closely related to the occurrence and metastasis of tumors. Therefore, we combined the anti-VEGF fusion protein conbercept, which is frequently used in the treatment of macular lesions, and the traditional chemotherapeutic drug doxorubicin (DOX). In order to reduce the frequency of drug administration and adverse drug effects and improve treatment compliance, we designed and successfully synthesized a pH-sensitive heptapeptide (DDIIIOH-NH$_2$) encapsulating conbercept and doxorubicin to form a stable hydrogel at a concentration of 20 mg mL^{-1} under pH 7.4. The hydrogel was characterized using transmission electron microscopy and rheological tests. Its drug-release properties under acidic and neutral conditions were also analyzed, with the results illustrating that the hydrogel had ideal solid stability, injectability, sustained-release behavior, and pH sensitivity. Meanwhile, the drug-delivery system effectively diminished Y79 tumor cells as well as inhibited the VEGF-induced proliferation of retinal endothelial cells (HRECs) and the following angiogenesis. *In vivo* experiments showed that the drug-delivery system could effectively inhibit the proliferation and angiogenesis of tumor tissues. We believe that the pH-sensitive hydrogel is an ideal drug-delivery system for the treatment of retinoblastoma.

1. Introduction

The clinical treatment of cancer has attracted widespread attention.[1–3] Retinoblastoma (RB), a malignant tumor originating from the retina, which frequently occurs in infants and children under 5 years of age, has main clinical symptoms such as leukocoria and loss of vision.[4–7] Current clinical treatments, including chemotherapy, cryotherapy, laser therapy, radiation therapy, and surgery, have mild or serious side effects.[8–15]

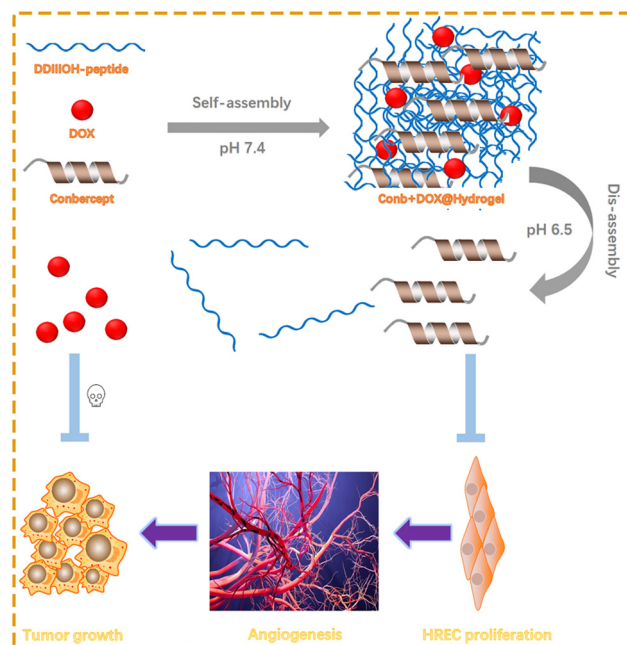Therefore, there is an urgent need to find an efficient and targeted therapy for RB.

Cytokines, such as vascular endothelial growth factor (VEGF), have been proven to be overexpressed in both RB aqueous humor and tissue and are associated with tumor angiogenesis and angiogenesis-related RB metastasis, nerve involvement, and RB differentiation.[16,17] Angiogenesis refers to the process of neovascularization from the existing vascular system by endothelial cells, which is regulated by stimulating or inhibiting the interaction between angiogenic factors.[18,19] Normal human vascular endothelial cells are in a resting state, while under certain specific pathological conditions, the endothelial cells could be activated and start proliferating. Tumor cells secrete a large amount of VEGF,[20] which acts directly on endothelial cells to promote the progress of angio-genesis and metastasis.[21] Judah Folkman called this regulatory effect of tumor cells a "vascular switching effect". Once the vascular switching effect is turned on, the growth of the tumor will not be restricted and corresponding invasion/metastasis ability will be significantly enhanced.[22–24] In recent years, inhibition of tumor angiogenesis has received increasing

[a] *Department of Ophthalmology, The First Affiliated Hospital of Nanjing Medical University, Nanjing, 210029, China*

[b] *School of Pharmacy, Shanghai Jiao Tong University, Shanghai 200240, China*

[c] *Shifa Tameer-e-Millat University Islamabad, Pakistan*

[d] *Nanjing iChemBridge Pharmaceutical Technology Co., Ltd, China*

[e] *The Affiliated Taizhou People's Hospital of Nanjing Medical University, Taizhou, 225300, China. E-mail: ymyspring@163.com*

[f] *School of Pharmacy, China Pharmaceutical University, Nanjing, 211100, China. E-mail: WuyiqunCPU@163.com; Tel: +86-15951715266*

† Electronic supplementary information (ESI) available. See DOI: https://doi.org/10.1039/d3ma01028g

attention in tumor treatment and several anti-angiogenic drugs targeting VEGF, such as bevacizumab (BVZ), have been widely used in clinical treatment.[9,25] These drugs can reduce tumor angiogenesis and normalize the survival of tumor blood vessels, thus cutting off oxygen and other nutrients needed for tumor cell growth and metastasis;[23] reduce the pressure between tumor tissues; improve the delivery of chemotherapeutic drugs to tumor tissues; and in turn enhance the efficacy of chemotherapy.[26] In the present study, we combined a VEGF inhibitor with the traditional chemotherapeutic drug doxorubicin to achieve better treatment of retinoblastoma, as the VEGF inhibitor can significantly reduce the angiogenesis of RB tissue derived from the retina, thus reducing the nutrition supply of tumor cells, ameliorating tumor metastasis, and reducing the pressure between tumor tissues, which is convenient for the drug permeation to exert a collaborative therapeutic effect with DOX. DOX can directly diminish tumor cells and alleviate the hypoxic/acidic tumor microenvironment.

Conbercept is an anti-VEGF fusion protein that is widely used in the clinical treatment of macular degeneration as it has high affinity with all subtypes of VEGF-A, VEGF-B, and placental growth factor.[27,28] Therefore, conbercept might be applied for the suppression of tumor angiogenesis through VEGF inhibition.[29] However, according to the manufacturer, the half-life of conbercept is only about 7 days. Although this is longer than the 4.25 days for bevacizumab,[30] it still cannot meet our goal to reduce the frequency of drug administration. Besides, doxorubicin is a traditional chemotherapeutic drug that has serious adverse reactions, such as bone marrow suppression and myocardial toxicity.[31] Hence it is necessary to find an ideal drug carrier for sustained and controlled release to achieve a better drug efficacy.

A hydrogel is a three-dimensional hydrophilic polymer gel with a high affinity for water and other body fluids, such as serum or plasma.[32] The concept of hydrogels has attracted attention in the biomedical field since the early 1960s. At that moment, Wichterle and Lim[33] prepared a synthetic hydrogel for biomedical applications. To date, hydrogels have been widely used in various biomedical fields, such as drug or cell delivery and tissue engineering, due to their good functionality, reversibility, and biocompatibility.[34–37] Based on whether they can change according to the changes in the external environment, hydrogels are divided into ordinary hydrogels and responsive hydrogels. While ordinary hydrogels are insensitive to environmental changes, the properties of responsive hydrogels (e.g., swelling behavior, structure, mechanical strength, permeability) could change under stimuli from external physical or chemical conditions.[38] When stimulated by temperature, light, mechanical stress, solvents, pressure, etc., a responsive hydrogel can change the sol–gel phase through reversible expansion or contraction of its own structure, thereby controlling the release of the drug.[39,40] Depending on the external stimuli, responsive hydrogels are mainly divided into temperature-, pH-, and photo-sensitive hydrogels.[41] Here, we designed a pH-sensitive polypeptide hydrogel encapsulating the VEGF inhibitor conbercept and the traditional

Scheme 1 Synthesis of the heptapeptide DDIIIOH. The peptide encapsulated conbercept and DOX to self-assemble into a stable hydrogel at pH 7.4. The hydrogel could then be embedded at the tumor site. The acidic tumor microenvironment led to an enhanced level of DDIIIOH protonation, leading to the disintegration of the hydrogel due to the strong electrostatic repulsion, which stimulated the release of conbercept and DOX. DOX was used to directly kill tumor cells, while conbercept could reduce the VEGF-induced HREC proliferation and angiogenesis in order to reduce the nutrition supply to the tumor and ameliorate tumor metastasis and reduce the pressure between tumor tissues, which is convenient for drug permeation to exert a collaborative therapeutic effect with DOX, enhancing the efficacy of chemotherapy. Furthermore, the inherent properties of the hydrogel could fundamentally alleviate adverse reactions caused by the systemic administration of chemotherapeutic drugs and reduce the frequency of drug administration, improving medication compliance for patients.

chemotherapeutic drug doxorubicin. We injected the hydrogel in to the peritumor and it intelligently responded to the lower pH to realize rapid and long-term drug release. Furthermore, the inherent properties of the hydrogel could fundamentally alleviate adverse reactions caused by the systemic administration of chemotherapeutic drugs and reduce the frequency of drug administration, improving medication compliance for patients, as shown in Scheme 1.

2. Materials and methods

2.1 Materials

Matrigel was purchased from Becton, Dickinson and Company (BD, USA). DDIIIOH peptide was synthesized by Nanjing SYN Company. HREC, Y79 cell lines were purchased from American Type Culture Collection (ATCC, USA). Human vascular endothelial growth factor (VEGF) was purchased from MedChemExpress. Cell Counting Kit-8 (CCK8) reagent and Bicinchoninic Acid Assay (BCA) reagent were purchased from Shanghai Yeasen. DOX was purchased from Sigma Aldrich. Conbercept

was purchased from Chengdu Kanghong Biotechnology Co., Ltd. RPMI-1640, DMEM medium, and fetal bovine serum (FBS) were purchased from Gibco. NOD/SCID mice were purchased from Cyagen Biosciences.

2.2 Synthesis of the peptide

The peptide (sequence: DDIIIOH-NH$_2$) was synthesized by Nanjing SYN Company through solid-phase polypeptide synthesis, including the connection between the C-terminal amino acid of polypeptide and Rink resin, extension of the peptide chains, cutting of the peptide chains, and purifying.

2.3 HPLC

Reversed-phase HPLC was selected to purify the peptide in the solid-phase synthesis. Polypeptide was dissolved by water. The solution was filtered by a 0.45 μm microporous membrane and purified with the Shimadzu LC-8A preparative RP-HPLC system. The chromatographic parameters were: use of a Shimadzu C18 column (4.6 × 250 mm, 5 μm), 0.1% TFA/water (V/V)-0.1% TFA/acetonitrile (V/V) as the mobile phase, flow rate of 5 mL min^{-1}, and elution time of 45 min. The purified peptide was obtained by freeze-drying.

2.4 Mass spectrometry

Liquid-mass spectrometry (LC-MS) was used to confirm the molecular weight of the target polypeptide after liquid-phase purification. The polypeptide solution with a concentration of 1 mg mL^{-1} was first prepared, and then the solution was filtered with a 0.22 μm aqueous microporous membrane. LC-MS analysis was used for the structural confirmation.

2.5 Preparation of peptide hydrogel

First, 0.2 mg doxorubicin hydrochloride was dissolved in 100 μL 10 mg mL^{-1} conbercept solution, and then 2 mg DDIIIOH-NH$_2$ polypeptide powder was dissolved in the aqueous solution, so that the concentrations of conbercept and DOX were 10 mg mL^{-1} and 2 mg mL^{-1}, respectively, and the final concentration of DDIIIOH peptide was 20 mg mL^{-1}. The pH value of the solution was adjusted to 7.4 with NaOH. A stable hydrogel was obtained within 5 min.

2.6 Transmission electron microscopy

Transmission electron microscopy (TEM) was used to observe the nano–microstructure of the peptides under different conditions. DDIIIOH polypeptide hydrogels at pH 7.4 and 6.5 were prepared. After stabilization, the hydrogel was crushed and suspended in H$_2$O. One drop of crushed hydrogel suspension was pipetted onto carbon-coated copper mesh, aspirating the excess liquid with filter paper after 3 min. Then, 2% phosphotungstate solution was added to the copper mesh for sample dyeing. After that, an HT-7700 type transmission electron microscope was used for observation and analysis of the peptide sample.

2.7 Rheological testing

Blank peptide hydrogel with a concentration of 20 mg mL^{-1} and another hydrogel loaded with conbercept and DOX were prepared. The experiments were performed with a HAAKE 600 rotary rheometer.

The parameters for the dynamic frequency sweep experiments were as follows: frequency of 0.1–10 rad s^{-1}, shear strain of 1%. The parameters for the dynamic time sweep experiments were as follows: frequency fixed at 6.28 rad s^{-1}; 0–120 s, shear strain of 1%; 120–240 s, shear strain of 50%; 240–360 s, shear strain of 1%. The total cycle lasted for 600 s.

2.8 *In vitro* drug release

The hydrogel was prepared according to Section 2.5. Here, 1000 μL PBS buffer (pH 7.4 and pH 6.5 and containing 1% phenylmethanesulfonylfluoride fluoride (PMSF)) was added as the release solution. The release solution was collected every 24 h and the same volume of fresh release solution was added to replace that taken out. Different concentrations of doxorubicin solution were tested and the absorbance of doxorubicin hydrochloride at 480 nm was recorded using a UV-vis spectrophotometer to draw a standard curve (Fig. S3, ESI†) (The UV/vis spectra of DDIIIOH, DOX, and conbercept are shown in Fig. S4 (ESI†), whereby 480 nm wavelength was used to detect the concentration of DOX, as DDIIIOH and conbercept had no absorbance at 480 nm). Different concentrations of conbercept solution were tested and BCA experiments were performed according to the manufacturer's instructions and used to plot the standard BCA curve (Fig. S2, ESI†). The collected release solution was observed at 480 nm with a UV-vis spectrophotometer and the absorbance was observed at 562 nm using a multifunctional microplate reader. The concentration of DOX or conbercept in the release solution was calculated, and the cumulative drug release curve was drawn according to the data obtained in the readings and calculations.

2.9 *In vitro* antitumor activity

Y79 tumor cells were seeded in a 96-well plate at a density of 5 × 10^3 per well. Conb@Hydrogel, DOX@Hydrogel, and Conb + DOX@Hydrogel were placed in 10 mL DMEM medium (pH 6.5 and 7.4) at 37 °C for 48 h and the medium was collected. Then, DMEM solution containing 0.1 mg mL^{-1} conbercept and 20 μg mL^{-1} DOX was prepared. All the solutions were filtered by a 0.22 μm sterile filter. The initial medium in the 96-well plate was discarded and 100 μL drug-containing DMEM solution prepared above was added. Next, 10 μL CCK-8 reagent was added to each well after 48 h. The OD value at the wavelength of 450 nm after incubation for 1.5–2 h was recorded.

$$\text{Relative cell viability (\%)} = (OD_{target} - OD_{blank})/(OD_{control} - OD_{blank}) \times 100\%$$

The concentration of the free drug was determined as follows: since the hydrogel encapsulated 1 mg conbercept and 0.2 mg DOX, if the drug was completely released in 10 mL release

solution, the concentration of conbercept was 0.1 mg mL^{-1} and the concentration of DOX was 20 μg mL^{-1}.

2.10 Study of the inhibitory effect of the drug-loaded hydrogels on VEGF-induced HREC proliferation

HRECs were seeded in 96-well plates at a density of 5×10^3 per well. After the cells were stabilized, 10% FBS DMEM was replaced with serum-free DMEM medium and the cells were starved for 24 h. The different masses of VEGF were then diluted with 10% FBS DMEM medium to obtain concentrations of 0, 5, 10, 20, 40, and 80 ng mL^{-1}, and the HRECs were incubated with DMEM containing VEGF for a total of 72 h. The CCK-8 assay was performed after the incubation.

2.11 Tube-formation experiment

Tube-formation experiments were performed to observe the effects of VEGF and anti-VEGF drugs on the formation of capillary-like structures. HRECs were treated as above. The matrigel was added in a pre-cooled 12-well plate and then placed in a 37 °C cell culture incubator for 30 min to solidify the matrigel. HRECs cultured for 72 h under various administrations were seeded on coagulated matrigel at a density of 1×10^6 per well. Cells were incubated for 6 h to form capillary-like structures. Images were taken using an inverted microscope. At least 7 random fields of view were picked to calculate the average number of branch points formed by the HRECs.

2.12 *In vivo* antitumor experiments

Twenty-five female NOD/SCID mice were purchased from Cyagen Biosciences with the age of six weeks. All the animal experiments were approved by the Ethics Committee of The First Affiliated Hospital of Nanjing Medical University (Jiangsu Province Hospital, Nanjing, China) and carried out in accordance with EC guidelines.

Y79 cells were resuspended using the medium and centrifuged at a speed of 1500 rpm for 5 min; then the supernatant was discarded and physiological saline was added to resuspend the cells. The cell density was controlled at 5×10^7 mL^{-1}. The right axillary skin of the mice was sterilized using 75% ethanol and then 0.1 mL cell resuspension was injected per mouse. The tumor-bearing mice were randomly divided into 5 groups when the tumor volume reached 150–200 mm^3. The administration was as follows: (1) control group: empty NOD/SCID mice were injected with 100 μL/20 g saline; (2) Conb@Hydrogel group: *in situ* injection of Conb@Hydrogel with the volume of 100 μL/20 g, where the dose of conbercept was equivalent to 50 mg kg^{-1}; (3) DOX@Hydrogel group: *in situ* injection of DOX@Hydrogel hydrogel with the volume of 100 μL/20 g, where the dose of DOX was equivalent to 10 mg kg^{-1}; (4) free Conb + DOX group: *in situ* injection of Conb + DOX solution with the volume of 100 μL/20 g, where the dose of conbercept was 50 mg kg^{-1} and the dose of DOX was 10 mg kg^{-1}; (5) Conb + DOX@Hydrogel group: *in situ* injection of Conb + DOX@Hydrogel with the volume of 100 μL/20 g, where the dose of conbercept was 50 mg kg^{-1} and the dose of DOX was 10 mg kg^{-1}. The administration day was viewed as day 0. The body weight were weighed at days 0, 2, 4, 6, 8, 10 and the tumor length (L) and width (W) were recorded using Vernier calipers. The calculation formula for the tumor volume was: $V \text{ (mm}^3) = L \times W^2/2$. On day 10, the mice were executed. Hematoxylin-eosin staining (H&E) was performed of the heart, liver, spleen, lung, kidney. Terminal deoxynucleotidyl transferase-mediated dUTP nick-end labeling (TUNEL) and CD31 immunohistochemistry (IHC) were also performed. The microvascular density (MVD) was analyzed using the Motic digital Slide Assistant System Lite 1.0. For detecting the histocompatibility and biodegradability, a blank hydrogel with the volume of 100 μL was embedded at the tumor site before weighing. After 10 days, the hydrogel was surgically removed for another weighing and then the biodegradable rate was calculated and the dissected skin tissue clinging to the hydrogel was collected for H&E staining.

3. Results and discussion

3.1 Design and synthesis of the peptide hydrogel

Under normal physiological conditions, polypeptides form conformations such as β-folding, β-corner, and twist into nanofibers at appropriate concentrations owing to their own properties, which can be used to encapsulate drugs or biological macromolecules. David *et al.*[42] reported a pentapeptide (sequence: DDIII) that had the ability to form a stable hydrogel. However, due to its poor solubility and pH-responsiveness, the polypeptide needed further modification. The pH-responsiveness of polypeptides to the microenvironment is mainly determined by the relationship between the pH and the pK_a value of amino acids. We introduced an alkaline amino acid-ornithine at the C-end of DDIII to make the side chain easier to be protonated. Meanwhile, the hydrophilic amino acid-histidine was added to improve the water solubility of the peptide. Furthermore, the imidazole ring structure of histidine provided stronger π–π interactions and in turn enhanced the self-assembly ability of the polypeptide. We used solid-phase peptide synthesis and selected Rink resin as the carrier to synthesize DDIIIOH polypeptide with 7 amino acids. HPLC showed that the purity was 97.23% (Fig. S1A, ESI†), and the mass spectrometry data showed that the molecular weight of the compound was consistent with the theoretical molecular weight of the polypeptide (Fig. S1B, ESI†), indicating the successful synthesis of the DDIIIOH peptide.

3.2 Characterization of the peptide hydrogel

As clearly shown in Fig. 1A, under pH 6.5, the hydrogel appeared to be in a liquid condition. It turned to a solid condition within 5 min after the pH was adjusted to 7.4. TEM was used to observe the state of the hydrogel in normal physiological environment (pH 7.4) and acid environment (pH 6.5) (Fig. 1B). At pH 7.4, the hydrogel presented a highly dense long fibrous structure with cavitary structures in the middle of the fiber so that the drug could be easily encapsulated in the hydrogel; while when the pH was adjusted to 6.5, the fiber structure completely disintegrated and the hydrogel
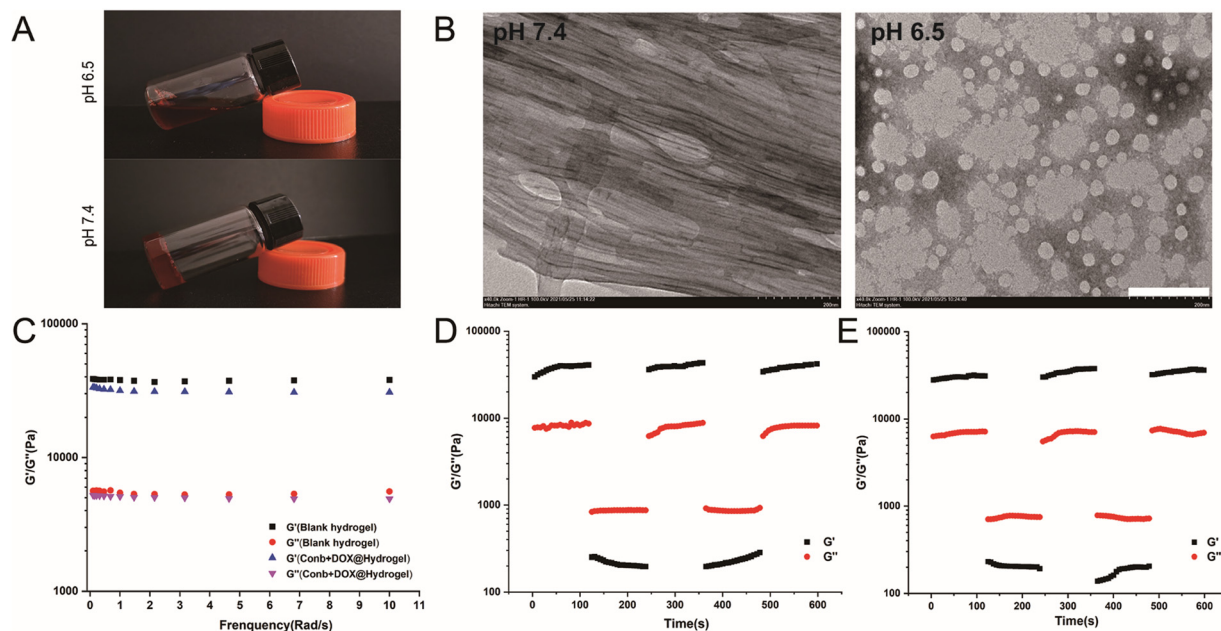
Fig. 1 Physical characteristics of the DDIIIOH peptide hydrogel. (A) Images of the DDIIIOH peptide hydrogel containing conbercept and DOX (Conb + DOX@Hydrogel) at pH 6.5 and 7.4. (B) TEM images of the blank DDIIIOH peptide hydrogel at pH 7.4 and 6.5. Scale bar: 200 nm. (C) Dynamic frequency scanning of the blank hydrogel and Conb + DOX@Hydrogel. (D) Dynamic time sweep of the blank hydrogel and Conb + DOX@Hydrogel (E).

structure appeared to have a loose spherical structure, indicating that the hydrogel had acidic sensitivity and the acidic microenvironment could completely destroy the three-dimensional network structure.

Rheology performance is an important indicator for examining the mechanical properties of hydrogels, which determines whether the hydrogel is stable and could be easily injected. The energy storage modulus, also known as elastic modulus, refers to the amount of the energy stored due to elastic deformation of a material when it undergoes deformation, reflecting the elastic size of the material. The energy consumption modulus, also known as the viscous modulus, refers to the material undergoing viscous deformation, where the amount of energy lost reflects the material's viscosity. When the energy storage modulus (G') is greater than the energy

consumption modulus (G''), it is considered that the material is solid. The dynamic frequency sweep results of the blank hydrogel and the loaded Conb + DOX@Hydrogel are shown in Fig. 1C. The G' values of the two hydrogels in the frequency range of 0.1–10 rad s^{-1} were 36109.29–43195.14 Pa and 34186.63–37186.68151Pa, while the values of G'' were 8277.65–8609.59 Pa and 7796.52–8099.61 Pa, respectively. There was no significant change in rheological properties before and after drug loading. The value of G' was about 5 times greater than the value of G'', proving that the hydrogel was a solid material with strong rigidity.

To verify whether the hydrogel would be easy to inject, we applied 1% strain for 120 s in the first stage and then applied 50% strain in the second stage for another 120 s, after which the strain immediately returned to 1%. The process lasted for
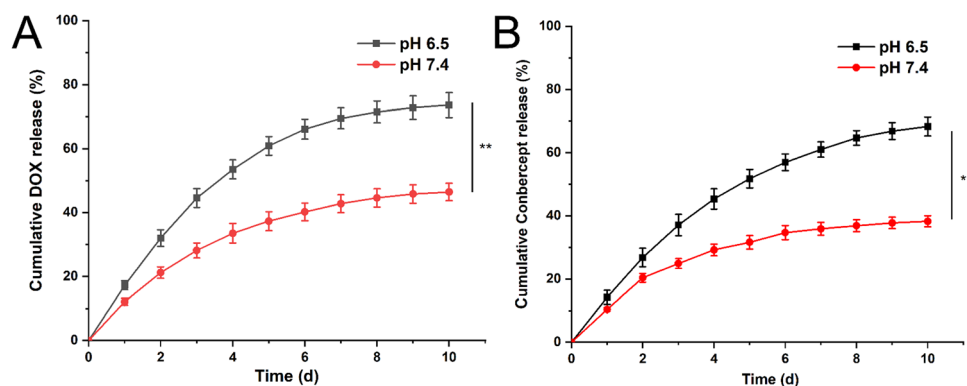

Fig. 2 Cumulative release curves for DOX (A) and conbercept (B) within 10 days at pH 6.5 and 7.4. Significant differences were analyzed using t-test, **, $p < 0.01$.

600 s. As shown in Fig. 1D and E, when the strain became 1%, the G' value became much higher than G'', proving that the hydrogel was solid. However, when the strain increased to 50%, the G'' value was higher than G', indicating that the hydrogel appeared to be liquid, and when the strain became 1% again, the values of G' and G'' were consistent with the first cycle, proving that the hydrogel presented a solid state when applying a small external force and showed a liquid state when a large external force was applied. More importantly, it could recover to a stable solid when the larger external force disappeared. To conclude, the hydrogel could be easily pipetted using a syringe and injected in to the tumor tissues.

3.3 In vitro drug release

We examined the ability of the hydrogel to release conbercept and doxorubicin (DOX) at pH 6.5 and pH 7.4. As shown in Fig. 2A, the cumulative release rate of DOX was 21.2% at pH 7.4 within 48 h; while under pH 6.5, the release rate reached 32.0%. The 10 day cumulative release rate showed a significant difference and its value was 46.4% at pH 7.4, and 73.6% under pH 6.5. For conbercept, the release rate at pH 7.4 was 20.4%, while it was 26.8% at pH 6.5 within 48 h. The 10 day cumulative release rate at pH 7.4 was 38.25% and at pH 6.5 it was 68.32%, respectively (Fig. 2B), illustrating the excellent pH sensitivity of the drug-loaded hydrogel. Compared with the release rate of DOX, the release rate of conbercept at the same time and same pH was relatively lower, and this phenomenon was possibly due to the larger molecular weight of conbercept as it could not be easily released from the hydrogel mesh structure.

3.4 Biocompatibility of the peptide hydrogel

Before validating the antitumor efficacy, we had to ensure that the hydrogel is biocompatible. Y79 cells and HRECs were incubated with 0, 1, 10, 50, 100, 500 $\mu g\ mL^{-1}$ peptide solution for 48 h. The CCK-8 results showed that the cell viabilities of Y79 cells and HRECs were all above 90%, and different concentrations of peptides had no significant effect on the cell viability of both cell lines (Fig. 3A). Next, we applied a time

gradient of 0, 12, 24, 48, 96 h to both cell lines at the concentration of 500 $\mu g\ mL^{-1}$. As shown in Fig. 3B, the cell viability was also greater than 90%. We thus believe that the peptide had excellent biocompatibility.

3.5 Antitumor efficacy in vitro

Y79 tumor cells were treated with free conbercept, free DOX, free conbercept + DOX, release solution of Conb@Hydrogel, release solution of DOX@Hydrogel, and release solution of Conb + DOX@Hydrogel for 48 h, respectively. The pH value of the medium was adjusted to 6.5 in all groups. As shown in Fig. 4, the survival rates of the free conbercept group and the Conb@Hydrogel group were 98.1% and 95.2% after 48 h, respectively. There was no significant difference with the control group, proving that conbercept had no adverse effect on Y79 tumor cells. The survival rate of the free doxorubicin group was only 3% and the survival rate of the free conbercept + DOX group was almost equal to that of the free DOX group. In the DOX@Hydrogel group, the cell survival rate was 15.7% due to the incomplete drug release, almost equal to that of the Conb + DOX@Hydrogel group. Although the inhibition rate was slightly lower than the free DOX group, it showed a significant difference compared with the control group, confirming that the drug-loaded hydrogel system had significant antitumor efficacy.

3.6 Anti-angiogenesis efficacy in vitro

Next, we examined the anti-angiogenesis efficacy of Conb@Hydrogel. Applying a gradient concentration of recombinant VEGF protein (0, 5, 10, 20, 40, 80 $\mu g\ mL^{-1}$) to HRECs for 72 h, as shown in Fig. 5A, with the increase in VEGF concentration, the proliferation rate of HRECs gradually increased. It had a particularly significant proliferative promotion effect on HRECs at concentrations of 40 and 80 ng mL^{-1}, confirming that VEGF did have the ability to promote the proliferation of HRECs. We thus selected 80 ng mL^{-1} as the suitable concentration for subsequent experiments.
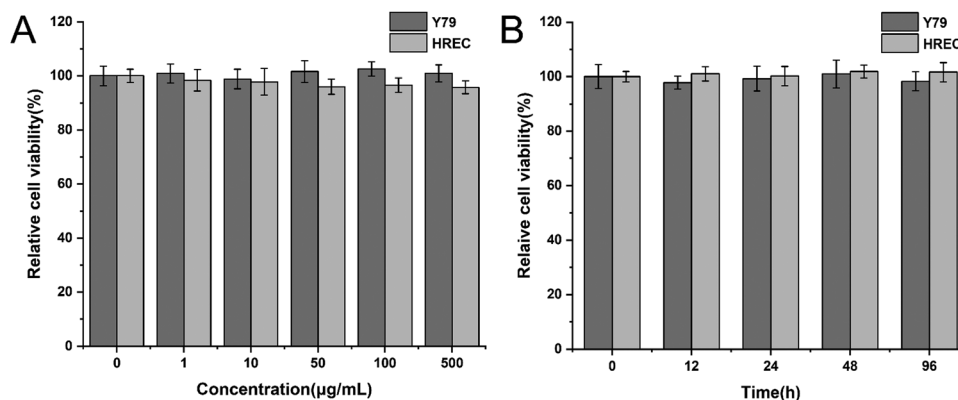

Fig. 3 Biocompatibility of the DDIIIOH peptide. (A) Relative cell viability of Y79 cells and HRECs treated with the DDIIIOH peptide with a concentration gradient of 0, 1, 10, 100, 500 $\mu g\ mL^{-1}$ for 48 hours. (B) Relative cell viability of Y79 cells and HRECs at concentrations of 500 $\mu g\ mL^{-1}$ for 0, 12, 24, 48, and 96 hours.
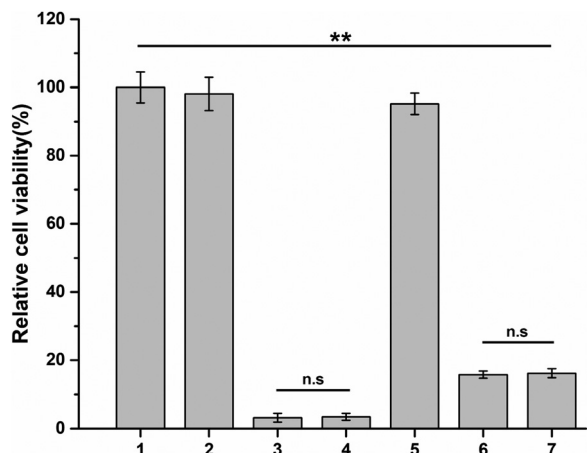
Fig. 4 Cytotoxicity of conbercept + DOX@Hydrogel. Relative cell viability of Y79 cells treated with blank DMEM medium, free conbercept (0.1 mg mL^{-1}), free doxorubicin (20 μg mL^{-1}), free conbercept + doxorubicin, Conb@Hydrogel, DOX@Hydrogel, and Conb + DOX@Hydrogel for 48 h; significant differences were analyzed using one-way ANOVA, n.s: no significance. **:$p < 0.01$. (1) Control, (2) free conbercept, (3) free DOX, (4) free conbercept + DOX, (5) Conbercept@Hydrogel, (6) DOX@Hydrogel, (7) conbercept + DOX@Hydrogel.

Then, we explored whether conbercept and Conb@Hydrogel could reverse VEGF-induced endothelial cell proliferation. As shown in Fig. 5B, the treatment of free conbercept (0.1 mg mL^{-1}) significantly reversed the effect of VEGF on HREC proliferation, while Conb@Hydrogel did not have such a significant reversal effect on proliferation due to the incomplete drug release. However, there were still significant differences compared with the free VEGF group and the value of cell viability was comparable to that of the control group. This result showed that the conbercept-loaded hydrogel could reduce the proliferation of endothelial cells induced by VEGF in pathological conditions.

We next investigated the inhibitory effect of Conb@Hydrogel on angiogenesis. As shown in Fig. 6A and B, the HRECs in the control group appeared to have a dense tubular structure and the number of tubular structures increased after the induction of 80 ng mL^{-1} VEGF. The number of tubular

structures decreased significantly after the addition of free conbercept or Conb@Hydrogel, confirming that the drug-delivery system had significant properties to inhibit angiogenesis.

3.7 Antitumor effect of the drug-loaded hydrogel *in vivo*

Furthermore, we evaluated the antitumor efficacy *in vivo*. The average weight changes of the mice in each group within 10 days is shown in Fig. 7A. We found that the body weight of the free DOX group was reduced to a certain extent that was significantly different from other groups, revealing that the hydrogel system had the function of the local sustained release of DOX, which in turn could improve the medication compliance. After examining the tumor volume curve and tumor anatomical diagram (Fig. 7B and C), we found that the tumor growth in the control group without drug treatment was extremely rapid, and the tumor volume quickly reached about 1700 mm^3 within 10 days. The antitumor efficacy of the Conb@Hydrogel group was obvious and the tumor volume within 10 days was only half that of the control group. However, the efficacy was still slightly worse than that of the DOX@Hydrogel group and free conbercept + DOX group, highlighting the excellent performance of DOX in inducing tumor cell death and showing that conbercept was not suitable for use as a medication alone. The Conb + DOX@Hydrogel group had the best antitumor efficacy and the average tumor volume was even smaller than the level before administration.

In the TUNEL staining experiments (Fig. 7D and E), the apoptosis rate of the control group tumor was only 0.82% and that of the Conb@Hydrogel group was 3.37%, indicating that the reduction of angiogenesis led to a decrease in the nutrient supply of tumor cells and then induced apoptosis. The apoptosis rate of the Conb + DOX@Hydrogel group was the highest and the value reached 21.52%, which was consistent with the results from the H&E staining (Fig. 7D). IHC was used to investigate the inhibitory effect of the administration system on tumor angiogenesis. CD31 staining of tumor blood vessels showed that the control group and the DOX@Hydrogel group
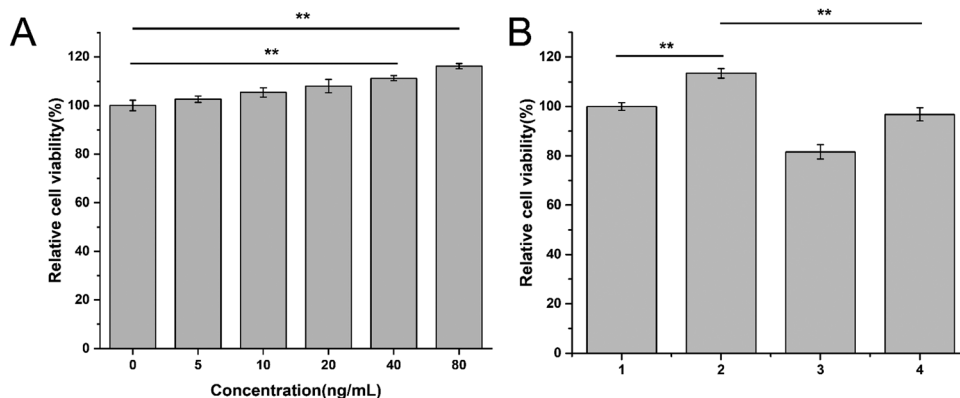

Fig. 5 (A) Relative cell viability of HRECs treated with dose-dependent VEGF for 72 hours. (B) Relative cell viability of HRECs treated with blank DMEM medium, VEGF, VEGF + free conbercept, and VEGF + Conbercept@Hydrogel for 72 hours; significant differences were analyzed by one-way ANOVA, *,$0.01 < p < 0.05$, **, $p < 0.01$. (1) Control, (2) VEGF, (3) VEGF + free conbercept, (4) VEGF + Conbercept@Hydrogel.
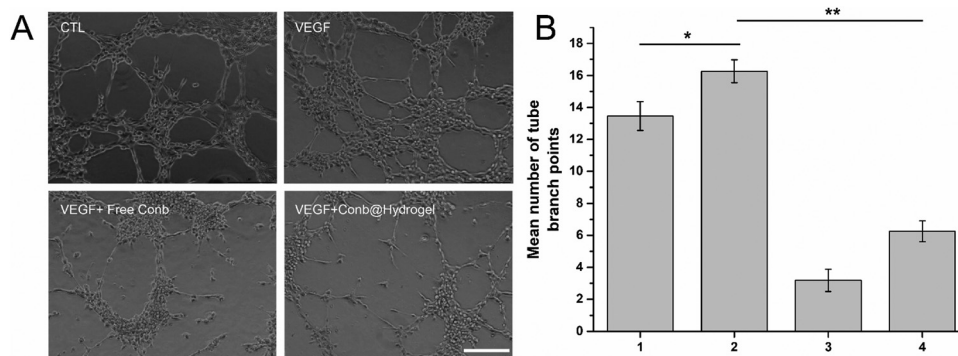
Fig. 6 Tube-formation experiments of HRECs. (A) Images of HRECs with different treatment methods for 6 hours; the images were taken by an inverted microscope (×400), scale bar is 250 μm. (B) Mean number of tube branches points calculated according to (A); significant differences were analyzed using one-way ANOVA, *, $0.01 < p < 0.05$, **, $p < 0.01$. (1) Control, (2) VEGF, (3) VEGF + free conbercept, (4) VEGF + Conbercept@Hydrogel.
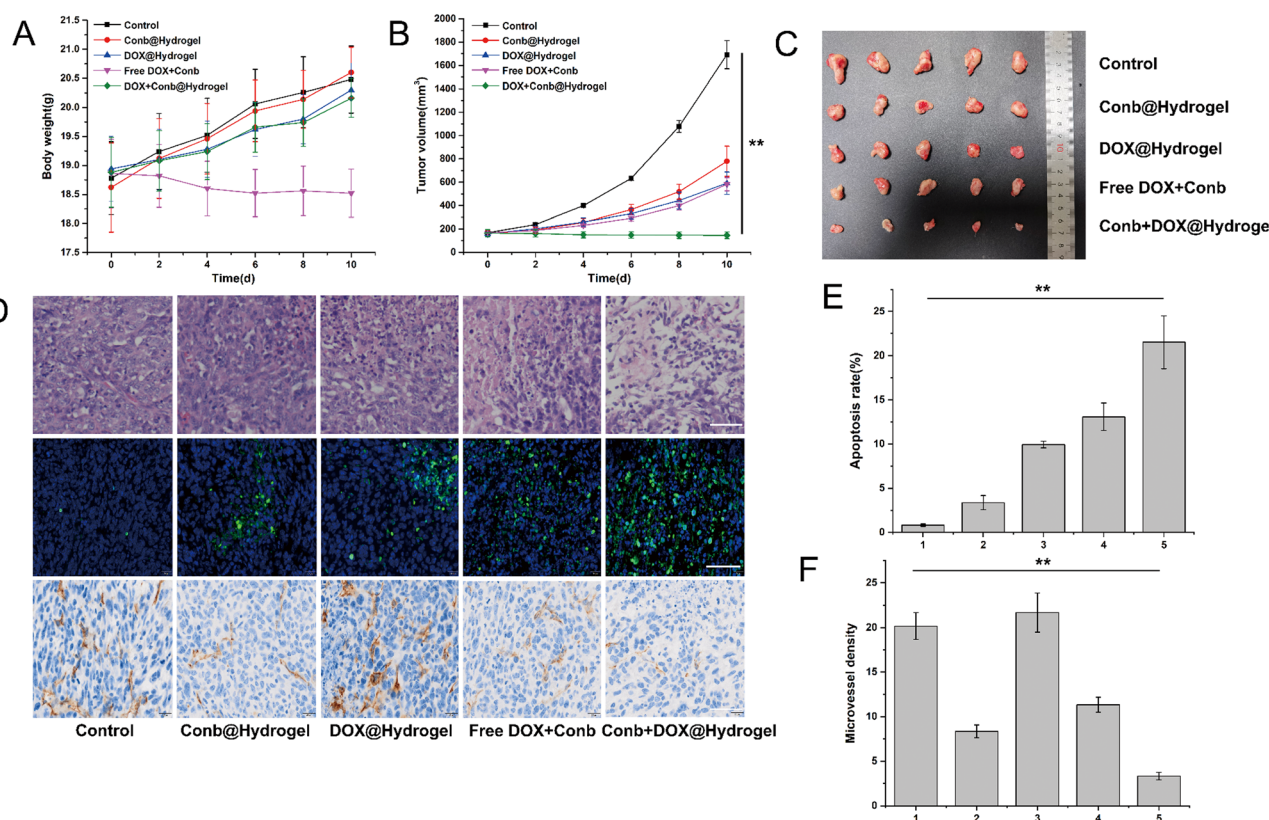

Fig. 7 Antitumor efficacy of Conb + DOX@Hydrogel in vivo. (A) Body weight, (B) tumor volume NOD/SCID tumor-bearing mouse within 10 days after administration. (C) Images of tumor issues collected at the end of drug administration. (D) TUNEL, H&E staining, and CD31 IHC staining of tumor tissues. Scale bar is 50 μm. (E) Statistical results of TUNEL staining, (F) statistical results of the CD31 IHC image representing the microvessel density (MVD); significant differences were analyzed uisng one-way ANOVA, **, $p < 0.01$. (1) Control, (2) Conbercept@Hydrogel, (3) DOX@Hydrogel, (4) free DOX + conbercept, (5) conbercept + DOX@Hydrogel.

had strong CD31 expression; while in the free conbercept + DOX group, CD31 expression was significantly reduced. The Conb@Hydrogel and Conb + DOX@Hydrogel groups had a fairly low CD31 expression and microvascular density, confirming that the sustained release of the hydrogel greatly improved the ability of conbercept to inhibit tumor angiogenesis.

H&E staining of the heart, liver, spleen, lung, and kidneys showed that the drug-delivery system did not damage healthy organs (Fig. S5, ESI†). Furthermore, the H&E staining of the skin tissues in the groups with hydrogel administration showed no necrosis or inflammation, which was similar to that of the control group (Fig. S6, ESI†) and the biodegradable rate of the hydrogel within 10 days was 61.7% ((99.17–37.98 mg)/

99.17 mg). The above results showed that the hydrogel drug-delivery system had excellent histocompatibility and biodegradability.

In summary, the combination of the angiogenesis inhibitor conbercept and the chemotherapeutic drug DOX and its implantation in a pH-sensitive peptide hydrogel could effectively inhibit tumor proliferation.

4. Conclusions

Solid-phase peptide synthesis was performed to synthesize a heptapeptide with the sequence DDIIIOH which self-assembled into a stable intelligent pH-responsive peptide hydrogel encapsulating the VEGF inhibitor conbercept and classic chemotherapeutic drug doxorubicin at a concentration of 20 mg mL^{-1} under pH 7.4. The peptide hydrogel had excellent stability, biocompatibility, and injectability. In the tumor microenvironment, the degree of protonation of the peptide was greatly enhanced, leading to a disintegration of the hydrogel due to electrostatic repulsion and the following rapid release of conbercept/doxorubicin, making sure that the drug-loaded hydrogel had excellent anti-angiogenesis and antitumor efficacies both *in vivo* and *in vitro*. In clinical RB treatment, the hydrogel delivery system would be directly injected into the corpus vitreum close to the tumor site to achieve efficient treatment. Moreover, the hydrogel system has the potential to act as a carrier for multiple drugs to cure various tumors and other diseases characterized with hypoxic microenvironments, such as rheumatoid arthritis.

Author contributions

Wen Fan performed the experiments. Mingkang Chen, Faisal Raza, Hajra Zafar, Faryal Jahan, Yuejian Chen and Lexin Ge help revise the manuscript. Minyan Yang supplied cell lines and NOD/SCID mice. Yiqun Wu designed and performed the experiments, wrote and revised the manuscript.

Ethical statement

All animal experiments approved by the Ethics Committee of The First Affiliated Hospital of Nanjing Medical University (Jiangsu Province Hospital, Nanjing, China) and carried out in accordance with EC guidelines.

Conflicts of interest

The authors declare that they have no competing financial interests or personal relationships that could have appeared to influence the work reported in this paper.

Acknowledgements

References

1 C. Xie, X. You, H. Zhang, J. Li, L. Wang, Y. Liu, Z. Wang, R. Yao, T. Tong, M. Li, X. Wang, L. Cui, H. Zhang, H. Guo, C. Li, J. Wu and X. Xia, A Nanovaccine Based on Adjuvant Peptide FK-13 and l-Phenylalanine Poly(ester amide) Enhances CD8(+) T Cell-Mediated Antitumor Immunity, *Adv. Sci.*, 2023, **10**(20), e2300418.

2 Y. Tao, C. Dai, Z. Xie, X. You, K. Li, J. Wu and H. Huang, Redox responsive polymeric nanoparticles enhance the efficacy of cyclin dependent kinase 7 inhibitor for enhanced treatment of prostate cancer, *Chin. Chem. Lett.*, 2023, 109170.

3 X. R. You, L. Y. Wang, J. F. Zhang, T. Tong, C. L. Dai, C. Chen and J. Wu, Effects of polymer molecular weight on *in vitro* and *in vivo* performance of nanoparticle drug carriers for lymphoma therapy, *Chin. Chem. Lett.*, 2023, **34**(4), 107720.

4 J. F. Chou, J. S. Ford, R. A. Kleinerman, D. H. Abramson, J. H. Francis, C. A. Sklar, K. C. Oeffinger, L. L. Robison, I. J. Dunkel and D. N. Friedman, General cancer screening practices among adult survivors of retinoblastoma: Results from the Retinoblastoma Survivor Study, *Pediatr. Blood Cancer*, 2021, **68**(4), e28873.

5 Z. Zhou, H. Jiang, J. Xia and J. Zhang, Comparison of the therapeutic effects of lobaplatin and carboplatin on retinoblastoma *in vitro* and *in vivo*, *Int. J. Oncol.*, 2020, **57**(3), 697–706.

6 H. Dimaras, E. A. Dimba and B. L. Gallie, Challenging the global retinoblastoma survival disparity through a collaborative research effort, *Br. J. Ophthalmol.*, 2010, **94**(11), 1415–1416.

7 S. Narang, A. Mashayekhi, D. Rudich and C. L. Shields, Predictors of long-term visual outcome after chemoreduction for management of intraocular retinoblastoma, *Clin. Exp. Ophthalmol.*, 2012, **40**(7), 736–742.

8 B. M. Faris, M. S. Tarakji, S. A. Baghdassarian and K. F. To'mey, The role of cryotherapy in the management of early lesions of retinoblastoma, *Ann. Ophthalmol.*, 1978, **10**(8), 1005–1008.

9 H. F. Darge, A. T. Andrgie, E. Y. Hanurry, Y. S. Birhan, T. W. Mekonnen, H. Y. Chou, W. H. Hsu, J. Y. Lai, S. Y. Lin and H. C. Tsai, Localized controlled release of bevacizumab and doxorubicin by thermo-sensitive hydrogel for normalization of tumor vasculature and to enhance the efficacy of chemotherapy, *Int. J. Pharm.*, 2019, **572**, 118799.

10 K. W. Mouw, B. Y. Yeap, P. Caruso, A. Fay, M. Misra, R. V. Sethi, S. M. MacDonald, Y. L. Chen, N. J. Tarbell, T. I. Yock, S. K. Freitag, J. E. Munzenrider, E. Grabowski, M. Katz, K. Kuhlthau, D. DeCastro, G. Heidary, J. Ciralsky, S. Mukai and H. A. Shih, Analysis of patient outcomes

following proton radiation therapy for retinoblastoma, *Adv. Radiat. Oncol.*, 2017, **2**(1), 44–52.

11 J. Li, Y. Zhang, X. Wang and R. Zhao, microRNA-497 over-expression decreases proliferation, migration and invasion of human retinoblastoma cells via targeting vascular endothelial growth factor A, *Oncol. Lett.*, 2017, **13**(6), 5021–5027.

12 R. Seth, A. Singh, V. Guru, B. Chawla, S. Pathy and S. Sapra, Long-term follow-up of retinoblastoma survivors: Experience from India, *South Asian J. Cancer*, 2017, **6**(4), 176–179.

13 R. Teixo, M. Laranjo, A. M. Abrantes, G. Brites, A. Serra, R. Proenca and M. F. Botelho, Retinoblastoma: might photodynamic therapy be an option?, *Cancer Metastasis Rev.*, 2015, **34**(4), 563–573.

14 C. L. Shields and J. A. Shields, Basic understanding of current classification and management of retinoblastoma, *Curr. Opin. Ophthalmol.*, 2006, **17**(3), 228–234.

15 H. M. Chen, S. J. Ong, A. N. Chao, K. L. Liou, S. M. Jung and L. Y. Kao, Histopathologic findings after selective ophthalmic arterial injection of melphalan for retinoblastoma, *Taiwan J. Ophthalmol.*, 2019, **9**(4), 262–266.

16 Y. Cheng, S. Zheng, C. T. Pan, M. Yuan, L. Chang, Y. Yao, M. Zhao and J. Liang, Analysis of aqueous humor concentrations of cytokines in retinoblastoma, *PLoS One*, 2017, **12**(5), e0177337.

17 B. K. Ghiam, L. Xu and J. L. Berry, Aqueous Humor Markers in Retinoblastoma, a Review, *Transl. Vis. Sci. Technol.*, 2019, **8**(2), 13.

18 P. Carmeliet and R. K. Jain, Molecular mechanisms and clinical applications of angiogenesis, *Nature*, 2011, **473**(7347), 298–307.

19 D. Hanahan and J. Folkman, Patterns and emerging mechanisms of the angiogenic switch during tumorigenesis, *Cell*, 1996, **86**(3), 353–364.

20 R. S. Apte, D. S. Chen and N. Ferrara, VEGF in Signaling and Disease: Beyond Discovery and Development, *Cell*, 2019, **176**(6), 1248–1264.

21 A. E. El-Kenawi and A. B. El-Remessy, Angiogenesis inhibitors in cancer therapy: mechanistic perspective on classification and treatment rationales, *Br. J. Pharmacol.*, 2013, **170**(4), 712–729.

22 J. Folkman, Tumor angiogenesis: therapeutic implications, *N. Engl. J. Med.*, 1971, **285**(21), 1182–1186.

23 J. Folkman, Antiangiogenesis in cancer therapy--endostatin and its mechanisms of action, *Exp. Cell Res.*, 2006, **312**(5), 594–607.

24 J. Folkman, E. Merler, C. Abernathy and G. Williams, Isolation of a tumor factor responsible for angiogenesis, *J. Exp. Med.*, 1971, **133**(2), 275–288.

25 E. Maj, D. Papiernik and J. Wietrzyk, Antiangiogenic cancer treatment: The great discovery and greater complexity (Review), *Int. J. Oncol.*, 2016, **49**(5), 1773–1784.

26 J. Pouyssegur, F. Dayan and N. M. Mazure, Hypoxia signalling in cancer and approaches to enforce tumour regression, *Nature*, 2006, **441**(7092), 437–443.

27 A. Y. Zhou, Y. J. Bai, M. Zhao, W. Z. Yu and X. X. Li, KH902, a recombinant human VEGF receptor fusion protein, reduced the level of placental growth factor in alkali burn induced-corneal neovascularization, *Ophthalmic Res.*, 2013, **50**(3), 180–186.

28 T. Li, A. Hu, S. Li, Y. Luo, J. Huang, H. Yu, W. Ma, J. Pan, Q. Zhong, J. Yang, J. Wu and S. Tang, KH906, a recombinant human VEGF receptor fusion protein, is a new effective topical treatment for corneal neovascularization, *Mol. Vision*, 2011, **17**, 797–803.

29 W. Fan, S. Li, J. Tao, C. Yu, M. Sun, Z. Xie, X. Wu, L. Ge, Y. Wu and Y. Liu, Anti-Vascular Endothelial Growth Factor Drug Conbercept-Loaded Peptide Hydrogel Reduced Angiogenesis in the Neovascular Age-Related Macular Degeneration, *J. Biomed. Nanotechnol.*, 2022, **18**(1), 277–287.

30 P. Bhattarai, S. Hameed and Z. Dai, Recent advances in anti-angiogenic nanomedicines for cancer therapy, *Nanoscale*, 2018, **10**(12), 5393–5423.

31 C. Carvalho, R. X. Santos, S. Cardoso, S. Correia, P. J. Oliveira, M. S. Santos and P. I. Moreira, Doxorubicin: the good, the bad and the ugly effect, *Curr. Med. Chem.*, 2009, **16**(25), 3267–3285.

32 D. Y. Fan, Y. Tian and Z. J. Liu, Injectable Hydrogels for Localized Cancer Therapy, *Front. Chem.*, 2019, **7**, 675.

33 S. Sharma and S. Tiwari, A review on biomacromolecular hydrogel classification and its applications, *Int. J. Biol. Macromol.*, 2020, **162**, 737–747.

34 Z. Zhang, Z. C. Hao, C. H. Xian, J. Y. Zhang and J. Wu, Triple functional magnesium ascorbyl phosphate encapsulated hydrogel: A cosmetic ingredient promotes bone repair via anti-oxidation, calcium uptake and blood vessel remodeling, *Chem. Eng. J.*, 2023, **472**, 145061.

35 G. Liu, Y. Zhou, Z. Xu, Z. Bao, L. Zheng and J. Wu, Janus hydrogel with dual antibacterial and angiogenesis functions for enhanced diabetic wound healing, *Chin. Chem. Lett.*, 2023, **34**(4), 107705.

36 P. Xin, S. Han, J. Huang, C. Zhou, J. Zhang, X. You and J. Wu, Natural okra-based hydrogel for chronic diabetic wound healing, *Chin. Chem. Lett.*, 2023, **34**(8), 108125.

37 Z. Xu, G. Liu, L. Zheng and J. Wu, A polyphenol-modified chitosan hybrid hydrogel with enhanced antimicrobial and antioxidant activities for rapid healing of diabetic wounds, *Nano Res.*, 2022, **16**(1), 905–916.

38 Y. Li, J. Rodrigues and H. Tomas, Injectable and biodegradable hydrogels: gelation, biodegradation and biomedical applications, *Chem. Soc. Rev.*, 2012, **41**(6), 2193–2221.

39 T. Vermonden, R. Censi and W. E. Hennink, Hydrogels for protein delivery, *Chem. Rev.*, 2012, **112**(5), 2853–2888.

40 F. Raza, H. Zafar, Y. Zhu, Y. Ren, A. Ullah, A. U. Khan, X. He, H. Han, M. Aquib, K. O. Boakye-Yiadom and L. Ge, A Review on Recent Advances in Stabilizing Peptides/Proteins upon Fabrication in Hydrogels from Biodegradable Polymers, *Pharmaceutics*, 2018, **10**(1), 16.

41 X. Li and X. Su, Multifunctional smart hydrogels: potential in tissue engineering and cancer therapy, *J. Mater. Chem. B*, 2018, **6**(29), 4714–4730.

42 D. E. Clarke, C. D. J. Parmenter and O. A. Scherman, Tunable Pentapeptide Self-Assembled beta-Sheet Hydrogels, *Angew. Chem., Int. Ed.*, 2018, **57**(26), 7709–7713.